JOURNAL OF MATERIALS SCIENCE 31 (1996) 3791–3803

The formation of TiC/Al_2O_3 microstructures by a self-propagating high-temperature synthesis reaction

C.R. BOWEN*, B. DERBY
Department of Materials, University of Oxford, Parks Road, Oxford, OX1 3PH, UK

The effect of processing variables on reaction rate and ceramic microstructure are examined for the self-propagating high-temperature synthesis reaction $3TiO_2 + 4Al + 3C \rightarrow 3TiC + 2Al_2O_3$. Reaction controlling methods used are reactant particle size, the use of diluents (to lower the combustion temperature) and the use of reactant preheating (to increase the combustion temperature). The ceramic microstructure has an unusual laminar structure which is generally only observed during unstable combustion wave propagation.

1. Introduction

Self-propagating high-temperature synthesis (SHS) is a processing technique which uses highly exothermic reactions to produce a variety of ceramic materials [1]. The technique begins by initiating an exothermic reaction in an area of a reactant mixture, e.g. with a resistively heated tungsten wire. Once initiated, there is sufficient heat release that the reaction becomes self-propagating. This leads to the formation of a combustion wave which travels along the reactants, converting them to the required products.

The potential advantages of SHS are that the process requires little energy and the processing time is reduced to seconds [2]. In addition, the high temperature of the combustion wave tends to expel many volatile impurities [3]. One of the major disadvantages of the process is that SHS produced ceramics are generally of high porosity unless some external means of densification, e.g. hot pressing, is employed [4].

With conventional sintering it is possible to have a degree of control over the microstructure, e.g. grain size and density, by altering the sintering profile. However, microstructural control is more difficult with SHS due to the high reaction rates. The aim of this paper is to discuss the influence of various processing parameters which could be used to control the reaction rate and hence the combustion wave velocity. In addition, the effect of these processing parameters on the final microstructure will be investigated.

The reaction under study is the aluminothermic reaction,

$$3TiO_2 + 4Al + 3C \rightarrow 3TiC + 2Al_2O_3 \quad (1)$$

which has previously been used to produce $TiC–Al_2O_3$ composites by a number of researchers [5–7].

Processing variables to be examined are the effect of reactant particle size, the use of diluents (to lower the combustion temperature) and the use of reactant preheating (to increase the combustion temperature).

2. Experimental technique

Powder blends of TiO_2 (particle size 0.63 μm, 98.7% purity from Johnson Matthey), Al (10.0 μm, 99.7%, ALPOCO) and carbon black (~0.02 μm, CABOT/Elftex 285) were produced by dry ball milling the powders with alumina media for 12 h. The reactant mixture was then sieved through a 100 μm mesh to reduce the number of agglomerates. Green bodies 30 mm × 15 mm and 5 mm thick were prepared by cold pressing at 40 MPa to approximately 50% theoretical density. The green bodies were then baked at 120 °C (in air) for 24 h to reduce the level of adsorbed water which would otherwise be violently expelled during the reaction.

Experiments were carried out in a transparent borosilicate glass tube under flowing Ar to prevent oxidation of the product TiC. The reaction was initiated by passing a current through the tungsten wire in contact with one end of the specimen. A camera with a high speed motor drive (2.5 frames s^{-1}) was used to measure the combustion wave velocity. Photographs were taken of the advancing combustion wave with a stopwatch visible in the picture to calculate the time difference between successive pictures (± 0.1 s). A distance scale was used to calculate the distance travelled by the wave (± 0.5 mm) at any time. Combustion wave velocities were measured from a minimum of three experimental runs.

To accurately measure the combustion wave velocity it was important to produce a planar combustion wave. It was observed that the tungsten wire initiated the reaction from a very small point in the sample causing the reaction wave to be curved as shown

* Currently at School of Materials, University of Leeds, Leeds, LS2 9JT, UK.

0022–2461

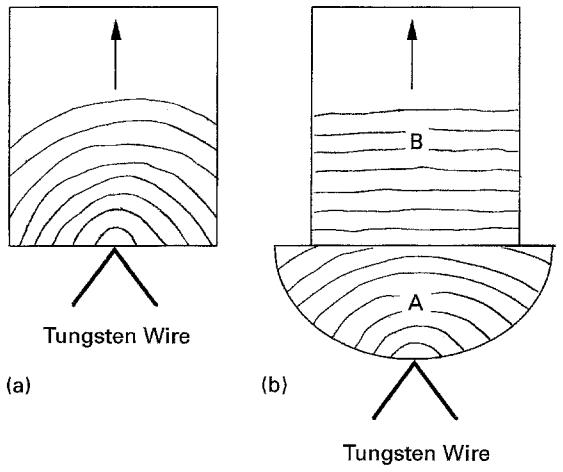

Figure 1 (a) Curved combustion wave produced by point ignition by a tungsten wire. (b) Experimental arrangement to produce a planar combustion wave.

schematically in Fig. 1a. By using the experimental configuration in Fig. 1b an approximately planar combustion wave is produced. The initiator sample (A) triggers the reaction along the complete edge of the sample of interest (B), producing a planar wave. It has been seen in the literature that many workers use large heat sources to initiate reactions in small samples. For example, Wrzesinski and Rawers [8] used an oxy-acetylene torch (3000 °C) to initiate a reaction in a sample 19 mm in diameter and 20 mm in height. It is likely that some preheating of the powder will occur before the reaction takes place and therefore the starting temperature of the powder is inhomogeneous and the combustion temperature will vary along the sample. By using the configuration shown in Fig. 1b, preheating of the sample before ignition is kept to a minimum.

The reaction is initiated by having the heated tungsten wire in contact with the reactant powder. This allows rapid heating and initiation of the reaction and reduces any preheating of the reactant powder away from the ignition point. This is preferred to reactions initiated by large tungsten wires which are not in contact with the compact and use radiative heating. Radiative heating provides a slower rate of heat transfer and increases the chance of preheating the reactant compact.

After synthesis reaction products were examined by X-ray diffraction (XRD). The microstructure was examined by optical microscopy (OM) and scanning electron microscopy (SEM). Product density was measured using Archimedes principle.

3. Results

The peak temperature of the combustion wave is estimated by calculating the adiabatic combustion temperature (T_{ad}). The calculation assumes that the enthalpy of the reaction heats up the products, and that no energy is lost to the surrounding environment. For Reaction 1, the adiabatic combustion temperature, calculated from Equation 2, is 2390 K which is above the melting point of Al_2O_3 (2323 K).

$$-3\Delta H_{r,298} = \int_{298}^{2323} C_p(3TiC + 2Al_2O_{3(s)})\,dT + \Delta H_f(2Al_2O_3) + \int_{2323}^{T_{ad}} C_p(3TiC + 2Al_2O_{3(l)})\,dT \quad (2)$$

where C_p is the heat capacity at constant pressure, ΔH_f is the latent heat of fusion and $\Delta H_{r,298}$ is the standard enthalpy of the reaction. For Reaction 1, $\Delta H_{r,298} = -357.4\,kJ\,mol^{-1}(TiO_2)$.

The combustion wave velocity for the $3TiO_2 + 4Al + 3C$ reaction was determined from the fast frame photographs of the advancing combustion wave and was calculated as $3.2 \pm 0.2\,mm\,s^{-1}$. The velocity did not vary significantly along the sample. The combustion temperature measured by a vanishing filament optical pyrometer was 2200 ± 200 K, below the adiabatic combustion temperature of 2390 K, as expected since heat losses occur.

XRD of the reaction products detected TiC and Al_2O_3 as seen in Fig. 2. No other products or residual reactants were detected. In addition to evolved gases, solids are also expelled during the reaction which can be seen to coat the Pyrex tube. A glass slide was placed above one specimen to collect the solids and XRD revealed that the solids were amorphous. The expelled solids may result from evaporation of carbon and other components at 2300 K followed by condensation.

The microstructure of the SHS produced TiC–Al_2O_3 ceramic is shown in Fig. 3a. The dark area is porosity and the white area is ceramic. It is observed that the products are highly porous and density measurement estimated the porosity level at $53 \pm 3\%$, which is similar to the initial green density. High porosity levels are common in SHS ceramic products due to the porosity forming mechanisms discussed by Rice and McDonough [4].

The sources of porosity are,

(i) porosity in the reactant green body,
(ii) outgassing of impurities during the high temperature reaction, e.g. H_2O,
(iii) the theoretical density of the product ($4360\,kg\,m^{-3}$) is higher than the theoretical density of the reactants ($3347\,kg\,m^{-3}$). As no significant change in sample dimensions was measured after synthesis, porosity was generated.

Although the products are highly porous the ceramic microstructure consists of an unusual regular laminar structure of alternating porosity and ceramic which has a spacing of approximately 90 μm. Laminar structures have previously only been observed when SHS reactions undergo spiral propagation, which is a form of unstable wave propagation [9]. To examine if the laminar structure is formed by the advancing combustion wave and is not a fabrication artefact, e.g. lamination of the reactants during compaction prior

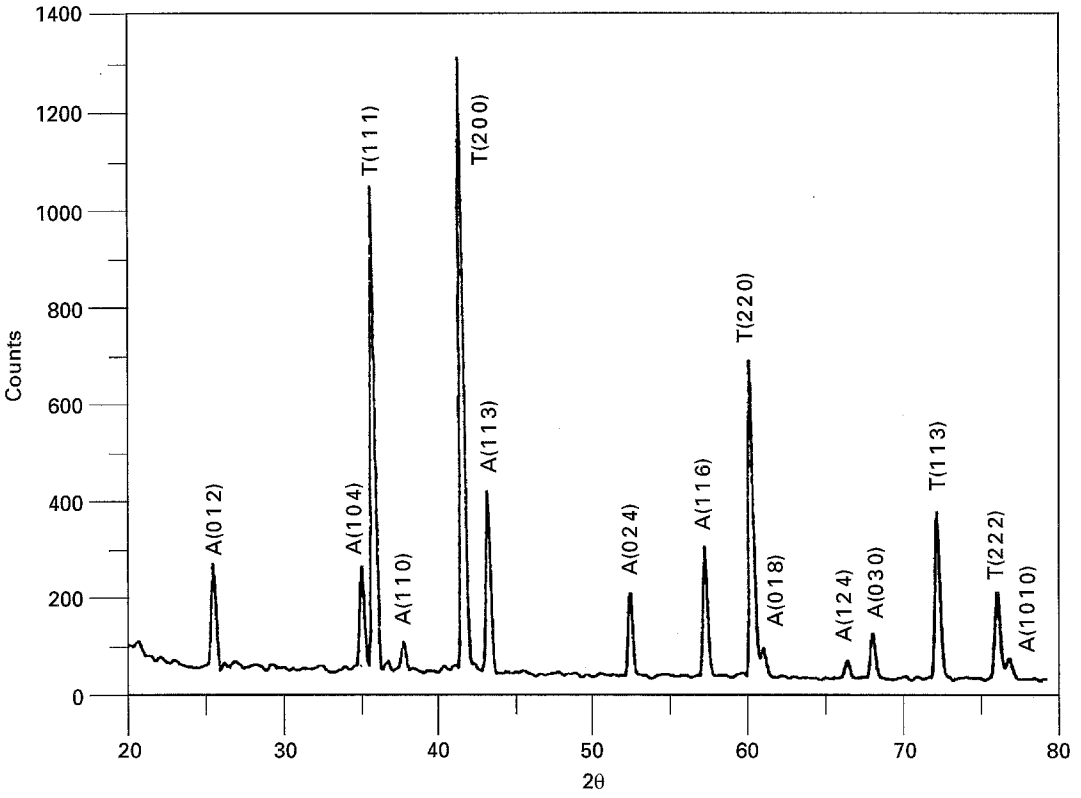

Figure 2 XRD of products showing TiC and Al_2O_3 formed by Reaction 1 (A = Al_2O_3 and T = TiC).

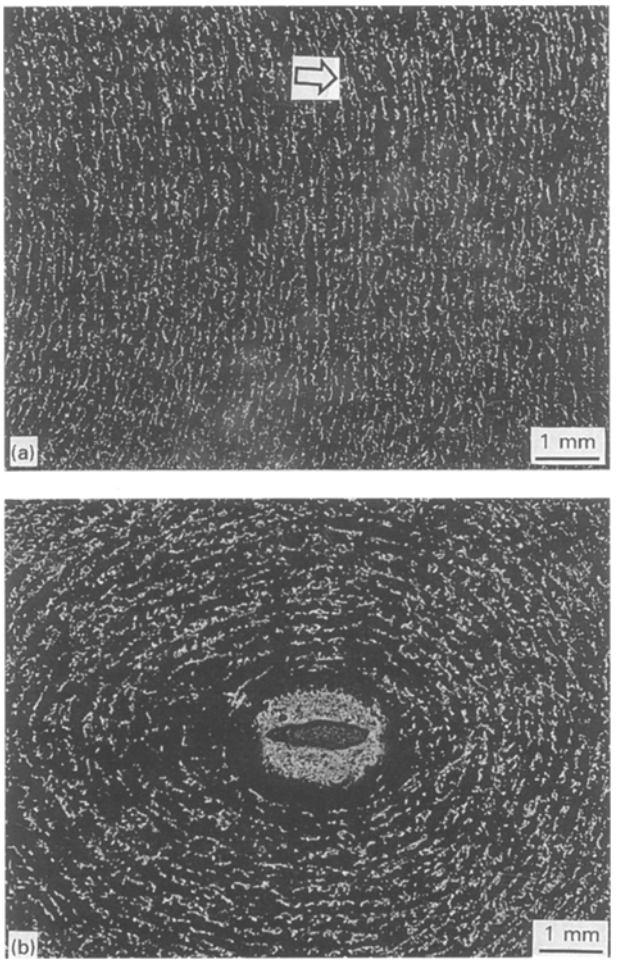

Figure 3 (a) Laminar microstructure produced by the combustion wave. Dark area is porosity and light area is ceramic. Direction of propagation is indicated by the arrow. (b) Circular microstructure produced via a spherical combustion wave.

to reaction, a spherical combustion wave was produced by initiating the reaction in the centre of the sample. The spherical combustion wave produces a corresponding spherical laminar microstructure which is shown by the characteristic circular pattern observed on the top surface of the specimen (Fig. 3b). Again the interlaminar spacing is constant throughout the sample.

4. Effect of reactant particle size on combustion wave velocity and microstructure

In solid–solid reactions it is expected that as the reactant particle size increases the rate of the reaction decreases, due to the larger product layer which forms between the reactant particles [10]. A variety of powders were used to examine the effect of particle size on the reaction rate and microstructure (Table I). The particle sizes were measured using laser scattering. The particle size of the carbon black powder could not be measured using this technique as the particles were too small, hence transmission electron microscopy was used.

The particle size of the reactants was varied by using the original reactant powder mixture (i.e. 10.0 μm Al, 0.63 μm TiO_2 and carbon black) as a standard. One of the reactants was chosen for study (e.g. Al) and the particle size was increased or decreased while the other reactants were kept constant (i.e. 0.63 μm TiO_2 and carbon black). The procedure was then carried out for the other two reactants. This allowed the individual examination of the effect of titania, aluminium and carbon particle size on reaction

TABLE I Various powders used as reactants

Powder	Purity (%)[a]	Source/code	Mean particle size (μm)
Al (atomized)	99.7	ALPOCO	8.3
Al (atomized)	99.7	Metalloys Ltd./1070	9.5
Al (atomized)	99.7	ALPOCO	10.0
Al (atomized)	99 min	Aldrich	46.0
TiO_2 (anatase)	99.95	Tioxide/RMS2	0.48
TiO_2 (anatase)	98.7 min	Johnson Matthey	0.63
TiO_2 (rutile)	99.9	Tioxide Specialties Ltd. High purity sandy rutile	17.1
C (amorphous)	–	Cabot Elftex 285 Fluffy	0.02
C (graphite)	–	Aldrich	7.2
C (graphite)	–	Wilson Graphite Powders OP LUX A 0484	14.9
C (graphite)	–	Wilson Graphite Powders BS 1762/6915	28.8
C (graphite)	99.5	Wilson Graphite Powders P (99.5/5)	45.3

[a] Purity as reported by manufacturer

rate and the microstructure of the ceramic. However, this did not investigate any synergistic influence of the particle sizes of different materials.

4.1. Aluminium particle size

Fig. 4 shows the combustion wave velocity as a function of aluminium particle size. The combustion wave velocity decreases with increasing particle size and the reaction fails to propagate with the 46 μm aluminium powder. The strong dependence of wave velocity with particle size was unexpected as the aluminium would be in the liquid phase during the reaction as the ignition temperature of the reaction (1173 K [11, 12]) is above the melting point of aluminium (932 K). This may be due to the fact that although the aluminium is molten it remains as a sphere of liquid aluminium retained by its surface oxide film.

The dependence of the microstructure on aluminium particle size is shown in Fig. 5. In the small range of 8–10 μm there is no significant change in the microstructure. However, when larger aluminium particles are used a regular laminar structure is not formed. This is primarily due to the unstable nature of the combustion propagation which was observed with aluminium particles greater than 10 μm.

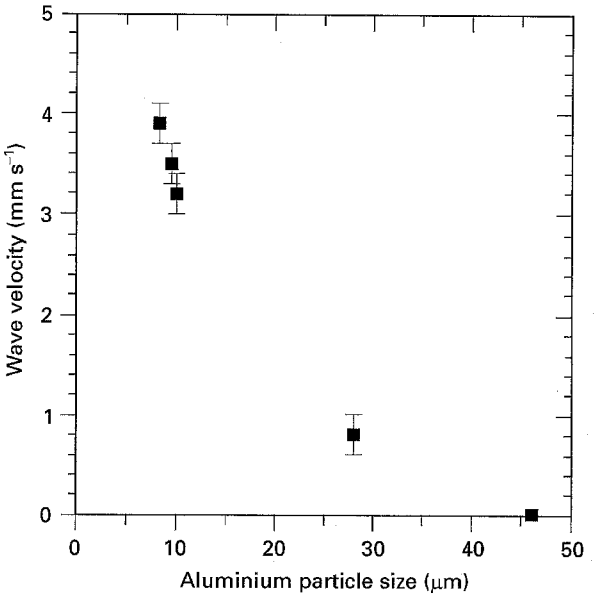

Figure 4 Graph of combustion wave velocity versus Al particle size.

4.2. Titania particle size

The variation of combustion wave velocity with titania particle size is shown in Fig. 6. As the particle size is increased the wave velocity decreases, due to the larger product layer which forms between the reactant particles. The variation in microstructure is shown in Fig. 7. For the small titania particle size (<1 μm) a laminar structure is observed. As the titania particle size is increased to 17 μm a randomly distributed porous structure is observed. The strong dependency of the ceramic microstructure on particle size may be due to the different combustion temperature attained by the ceramic with different particle size. The effect of titania particle size on the combustion temperature of Reaction 1 has been studied by Feng and Moore [13] who examined various TiO_2 powder sizes in the range 50–200 μm. Pyrometer measurements indicated that as the reactant particle size increased the combustion temperature decreased, presumably due to the reaction taking place over a longer time and thus heat losses becoming more significant. Therefore, as the titania particle size is increased from <1 to 17 μm the combustion temperature may decrease to produce the different microstructures.

4.3. Carbon particle size

The variation of carbon particle size with wave velocity is shown in Fig. 8a. The wave velocity is shown to initially "*increase*" when the carbon particle size increases from the 0.02 μm carbon black to the 7.2 μm

graphite powder. Further increase in the carbon particle size then leads to a decrease in wave velocity with the reaction failing to propagate at a particle size of 45 μm.

The increase in wave velocity may be explained from observations of the colour of the reactant compacts. When the small 0.02 μm carbon black particles are present the reactant compact is black as the carbon particles coat the larger 0.63 μm titania and 10 μm aluminium particles. When the 7 μm graphite particles are used it is the titania which has the smallest particle size and therefore the titania phase is continuous, resulting in a white reactant compact. These different particle arrangements can have two effects on the reaction rate. Firstly, the thermal conductivity of the compact is expected to increase when the titania becomes the continuous phase. The thermal conductivity is no longer dominated by the low

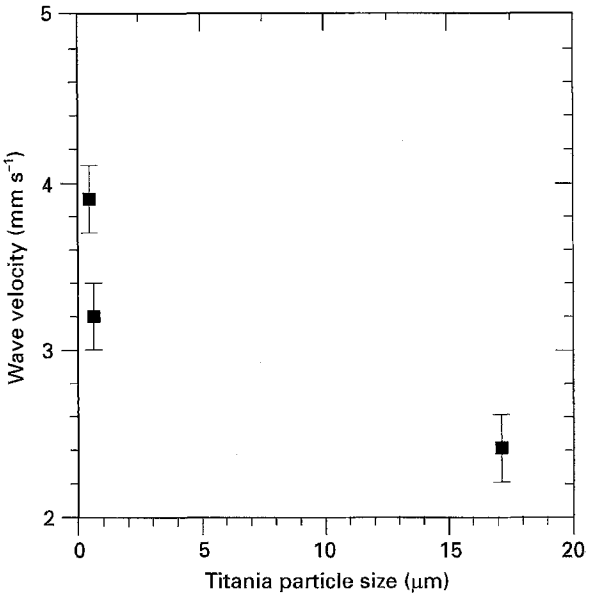

Figure 6 Graph of combustion wave velocity versus TiO_2 particle size.

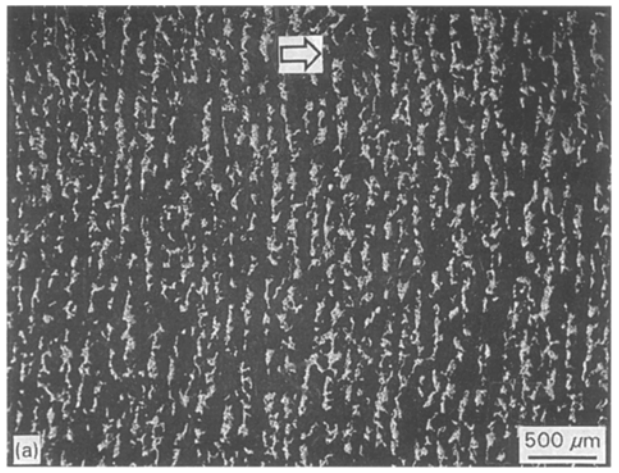

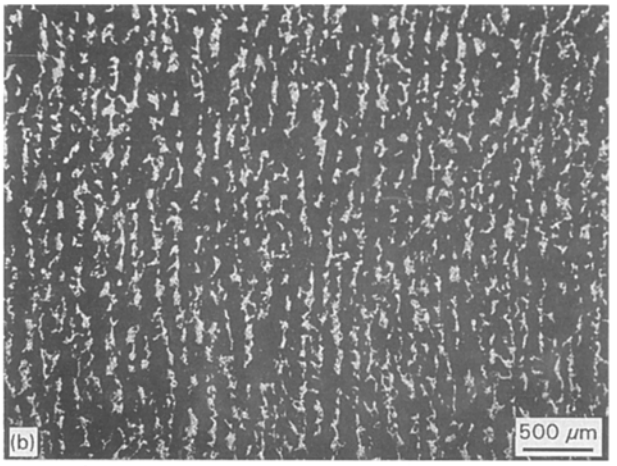

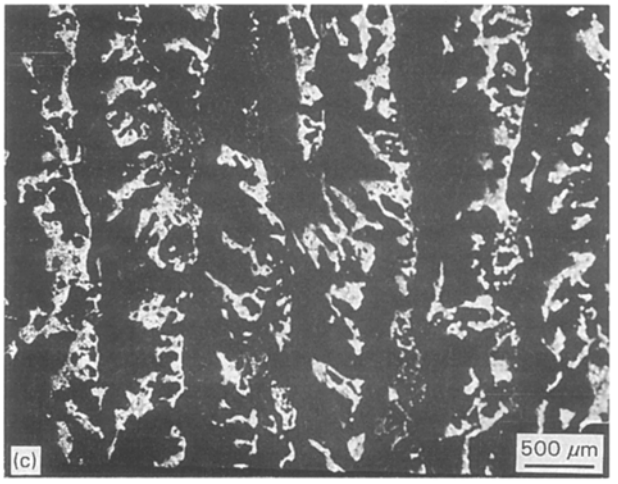

Figure 5 $TiC–Al_2O_3$ microstructures using TiO_2 (particle size 0.63 μm), carbon black (0.02 μm) and various Al particle sizes. (a) 8.3 μm, (b) 10.0 μm and (c) 28 μm.

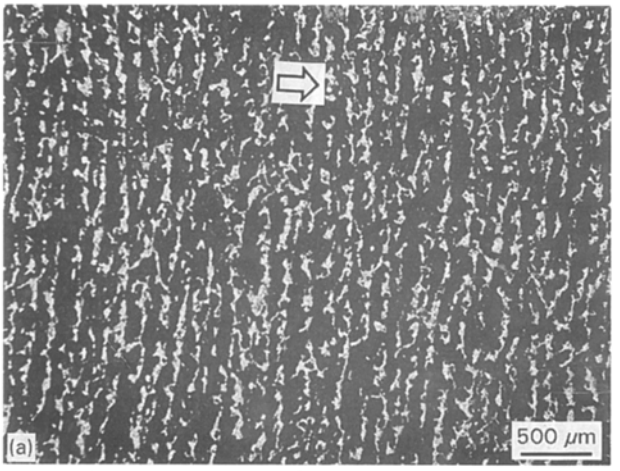

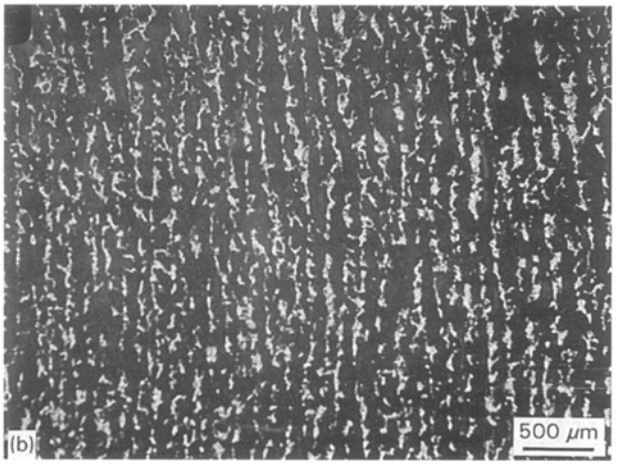

Figure 7 $TiC–Al_2O_3$ microstructures using Al (particle size 10.0 μm), carbon black (0.02 μm) and various TiO_2 particle sizes (a) 0.48 μm, (b) 0.63 μm and (c) 17.3 μm.

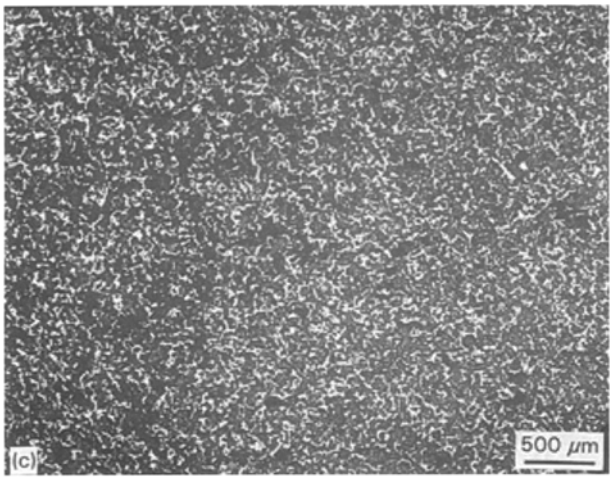

Figure 7 (Continued).

thermal conductivity of the carbon black phase. In addition it is believed, from thermal analysis measurements [11], that the reaction is initiated by a reaction between titania and aluminium. The sequence of reactions is thought to be,

(i) the aluminium phase melts and reacts with the titania

$$3TiO_2 + 4Al \rightarrow 3Ti + 2Al_2O_3 \qquad \text{at } 900\,^{\circ}C$$

(ii) the titanium reacts with the free carbon

$$Ti + C \rightarrow TiC$$

to produce the $TiC–Al_2O_3$ ceramic composite.

Fig. 8b shows that when the carbon black is a continuous phase it may be possible for the carbon to act as a barrier to titania–aluminium particle contact, which is necessary for the initial reaction to TiO_2 and Al. However, when the titania is continuous the aluminium–titania particle contact is greater which may lead to the increased wave velocity.

Fig. 9 shows the change of the ceramic microstructure with carbon particle size. As observed with the aluminium and titania particles, the laminar structure disappears on increasing the particle size. As larger particles are used, cracking of the product is also more common. This may be due to larger particles reducing the combustion temperature to below the melting point of the alumina phase as was reported by Feng and Moore [13] with TiO_2 particle size. This effect has also been observed when diluents have been used to control reaction rates.

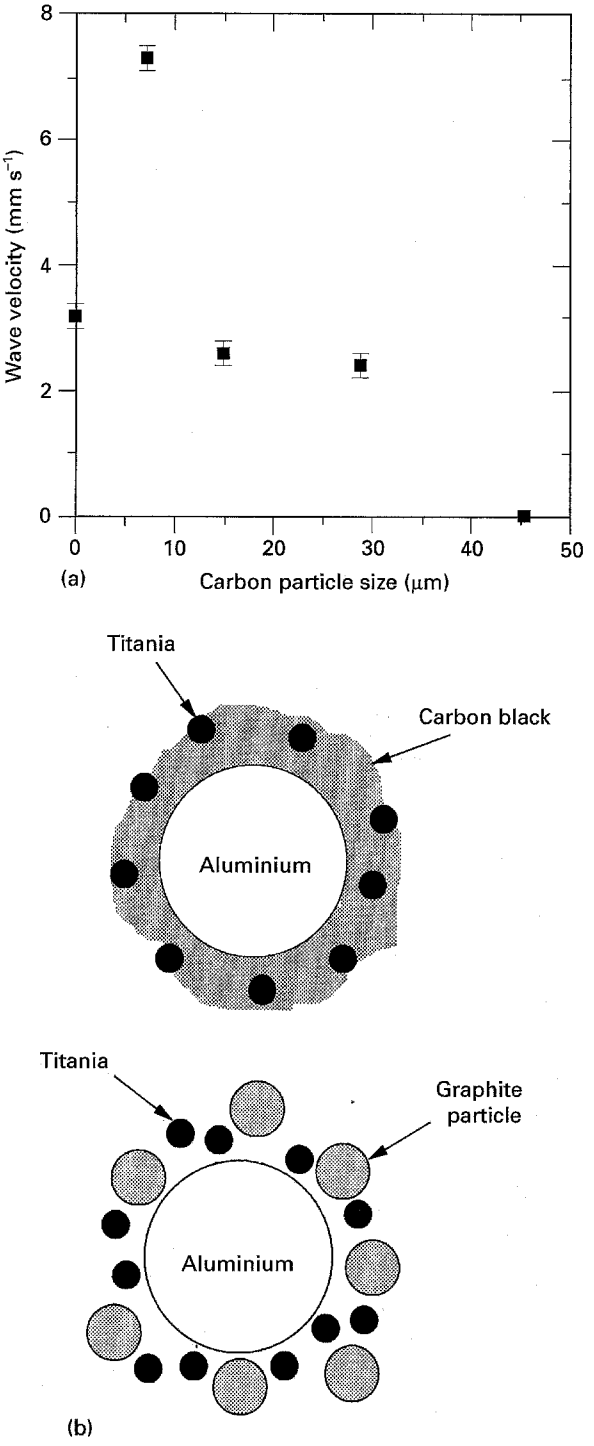

Figure 8 (a) Graph of combustion wave velocity versus carbon particle size. (b) Schematic showing how small carbon black particles act as a barrier to TiO_2–Al particle contact.

5. Effect of diluents on combustion wave velocity and microstructure

Another possible method of attempting to control the SHS reaction is by adding diluents to the reactants which lowers the adiabatic combustion temperature. For example, some of the products of an SHS reaction can be added to the initial reactants. These additions do not take part in the reaction but they increase the thermal mass of the system and lower the adiabatic combustion temperature. The lowering of the adiabatic combustion temperature would result in a decrease in the reaction rate and the combustion wave velocity [14, 15].

5.1. Addition of reaction products (Al_2O_3)

Alumina powder of mean particle size 0.7 μm was added to the initial reactants of Reaction 1. The reaction is now,

$$3TiO_2 + 4Al + 3C + xAl_2O_3 \rightarrow 3TiC + (2 + x)Al_2O_3. \qquad (3)$$

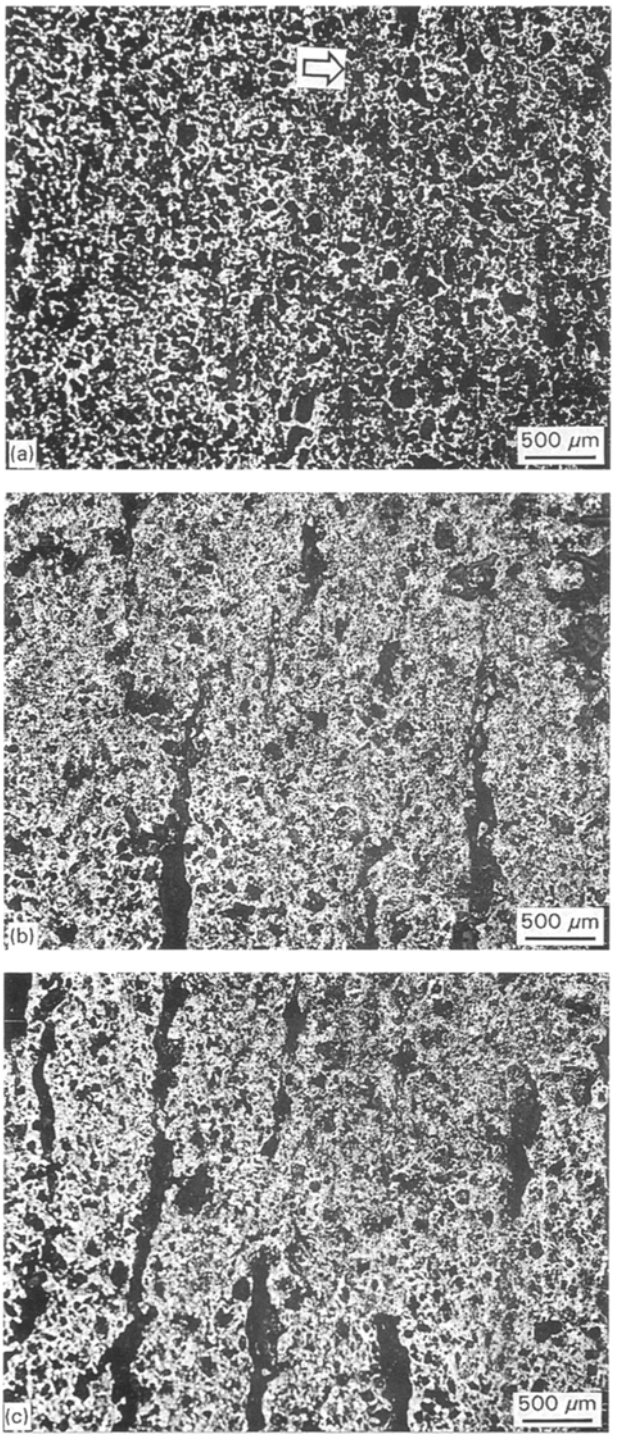

Figure 9 TiC–Al_2O_3 microstructures using Al (particle size 10.0 μm), TiO_2 (0.63 μm) and various carbon particle sizes (a) 7.2 μm, (b) 14.9 μm and (c) 28.8 μm.

The reactant mixtures were prepared as before but now containing 5 wt % ($x = 0.198$ mole in Reaction 3), 10 wt % ($x = 0.418$), 15 wt % ($x = 0.664$) and 20 wt % ($x = 0.941$) of Al_2O_3. In addition to reducing the combustion temperature, the Al_2O_3 particles may also act as a barrier to reactant particle contact.

The addition of the diluent leads to a decrease in the combustion temperature and wave velocity as seen in Fig. 10. At 20 wt % Al_2O_3 the combustion temperature is not sufficient to produce a propagating wave.

The use of alumina diluent has allowed the wave velocity and the reaction rate to be controlled. This could lead to the possibility of controlling the ceramic

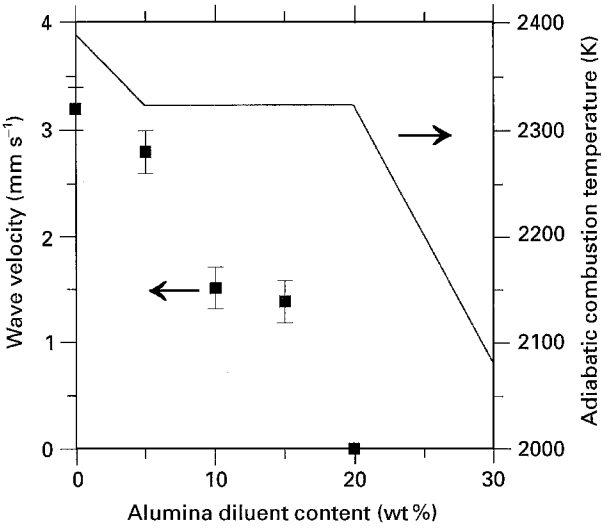

Figure 10 Graph of combustion wave velocity and calculated adiabatic combustion temperature versus Al_2O_3 diluent content.

microstructure. Fig. 11 shows that increasing the alumina diluent content produces severe cracking of the ceramic. The reason for the cracking may be that as the diluent level increases the actual combustion temperature is lowered below the melting point of the alumina phase. There is no liquid phase present during the reaction to relieve thermal stresses which develop in the ceramic during the high temperature reaction. The unrelieved thermal stress could cause the cracking and delamination of the ceramic. It was therefore decided to use aluminium as a diluent as it would remain in the liquid phase during the reaction and during cooling of the product to relatively low temperatures.

5.2. Addition of excess reactants (Al)

In order to use aluminium as a diluent, excess aluminium powder was mixed with the powder reactants. The reaction is now,

$$3TiO_2 + (4 + y)Al + 3C \rightarrow 3TiC + 2Al_2O_3 + yAl \quad (4)$$

which produces a ceramic–metal composite. This reaction has been investigated by Feng *et al.* [16] who attempted to use the liquid aluminium phase to infiltrate the porous ceramic and produce a dense product. Samples consisting of 5 wt % ($y = 0.75$ mole), 10 wt % ($y = 1.58$), 15 wt % ($y = 2.51$), 20 wt % ($y = 3.55$), 30 wt % ($y = 6.09$) and 40 wt % ($y = 9.46$) addition of excess aluminium were prepared. The experimental measurements of the variation of wave velocity and adiabatic combustion temperature with aluminium content are shown in Fig. 12. The wave velocity increases with a small addition of excess aluminium (5 wt %) and then begins to decrease at higher additions of diluent with the reaction failing to propagate at 40 wt % excess aluminium. An increase in wave velocity with increasing liquid diluent has been observed by Fu *et al.* [17] with $Ti + 2B + xAl \rightarrow TiB_2 + xAl$. The possible reason for the increased

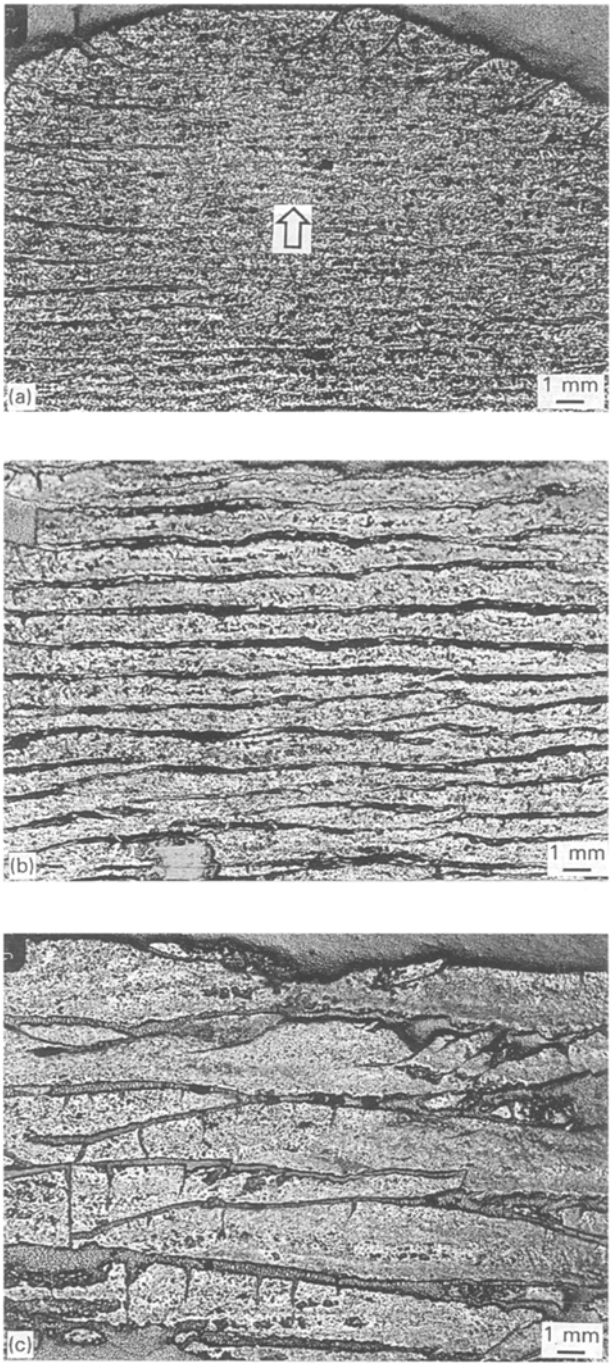

Figure 11 TiC–Al_2O_3 microstructures using Al_2O_3 as a diluent to control the reaction rate (a) 5 wt %, (b) 10 wt % and (c) 15 wt %.

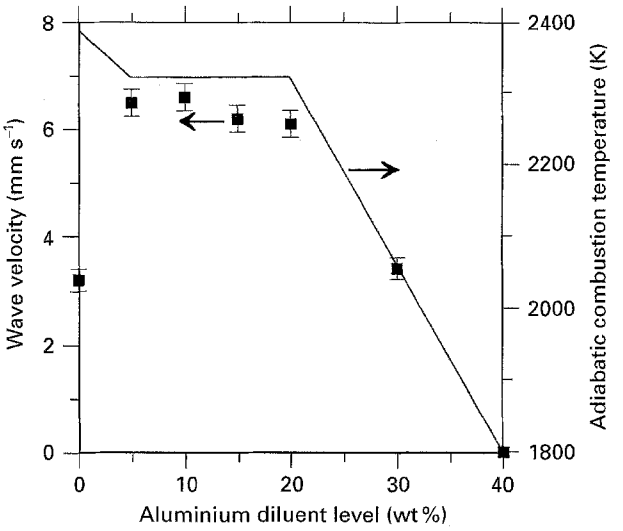

Figure 12 Graph of combustion wave velocity and calculated adiabatic combustion temperature versus Al diluent content.

combustion wave velocity was thought to be the increased mass diffusion and heat transfer in the presence of a liquid phase which wets the solids, increasing the contact area.

X-ray diffraction of the product revealed that a TiC–Al_2O_3–Al composite was formed and that no other compounds, such as Ti aluminides, were detected. Only at 30 wt % Al where the wave velocity was low and unstable was any cracking observed. The lack of cracking with up to 20 wt % Al may be associated with the liquid phase allowing thermal stresses to be relieved during cooling, or else the presence of large volumes of ductile metal providing the same function.

The microstructure of the ceramic as the aluminium content increases is shown in Fig. 13. It can be seen that the laminar structure of the product is retained with additions of 5 to 20 wt % excess aluminium. The laminar structure and the scale of the laminar structure is not effected by the presence of the liquid Al phase nor by the "*speed*" of the combustion wave which varies considerably between 0–20 wt % added Al. At 30 wt % the wave becomes unstable and the product microstructure becomes irregular as seen in Fig. 13g.

The liquid aluminium has little effect on the laminar structure which is very different to the effects observed when Al_2O_3 was used as a diluent. This observation may indicate that a liquid phase is important in the mechanism which produces the laminar structure. The liquid aluminium does not fill the porosity between the laminates to a large extent (Fig. 13) but it does infiltrate the ceramic laminates as seen by the SEM photographs in Fig. 14, which are fracture surfaces perpendicular to the direction of propagation. As the aluminium content increases the density of the ceramic laminates increases as the liquid aluminium infiltrates the pores.

6. Effect of preheating

The final method of attempting to control the SHS process is achieved by heating the reactants prior to ignition of the combustion wave. Whereas diluents are used to decrease the adiabatic combustion temperature, preheating the reactants results in an increased adiabatic combustion temperature [1, 18]. The increased T_{ad} increases the reaction rate and combustion wave velocity. The preheating temperature has been shown to have a significant effect on the microstructure of the ceramic formed [19]. Preheating has also been used to react less exothermic reactions which do not usually undergo SHS [20].

The preheating apparatus was constructed from a modification of the experimental equipment designed for room temperature ignition. The reactant compact was placed on a graphite base and positioned

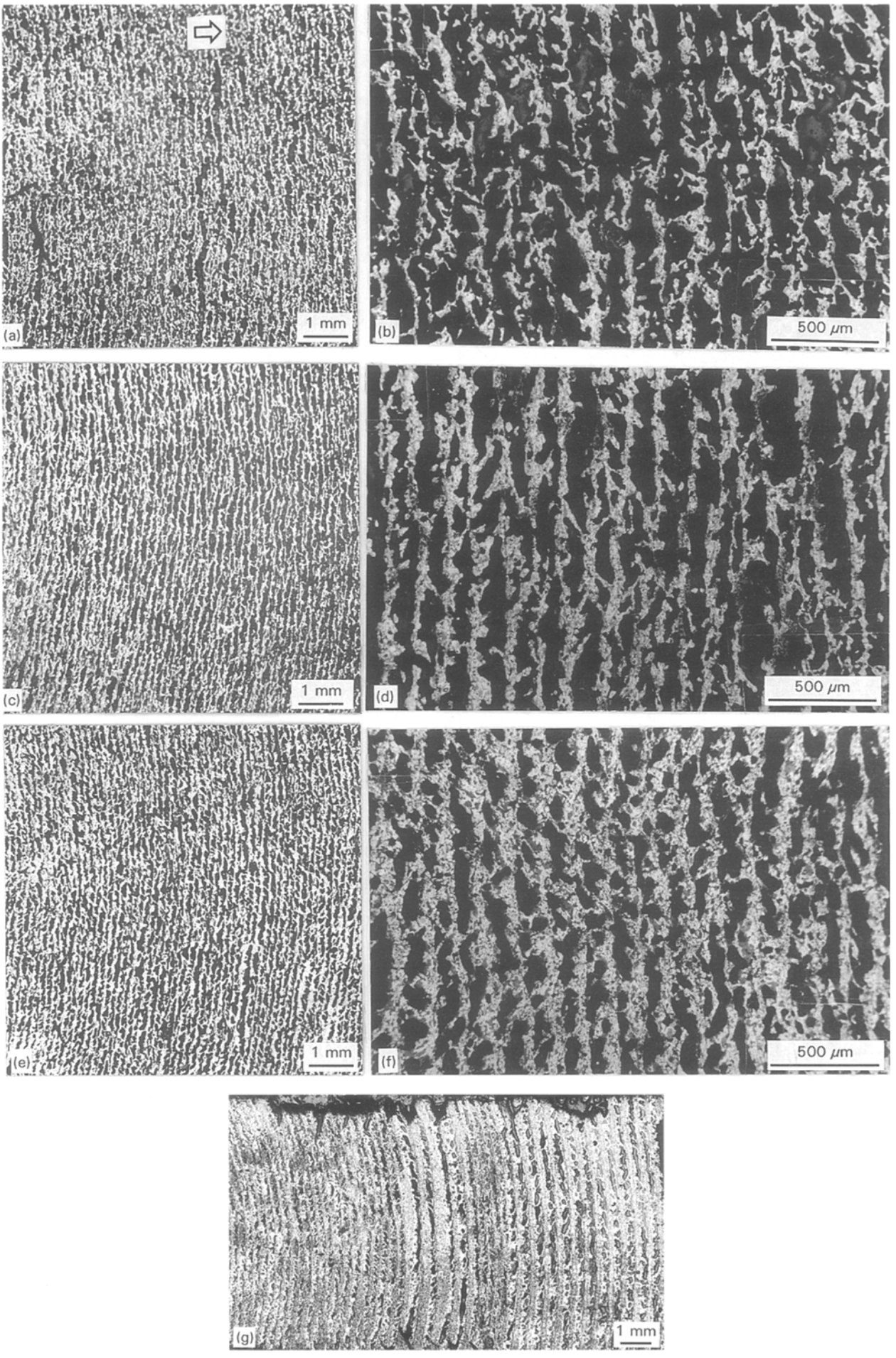

Figure 13 TiC–Al_2O_3 microstructures using Al as a diluent to control the reaction rate (a) and (b) 5 wt %, (c) and (d) 10 wt %, (e) and (f) 20 wt % and (g) 30 wt %.

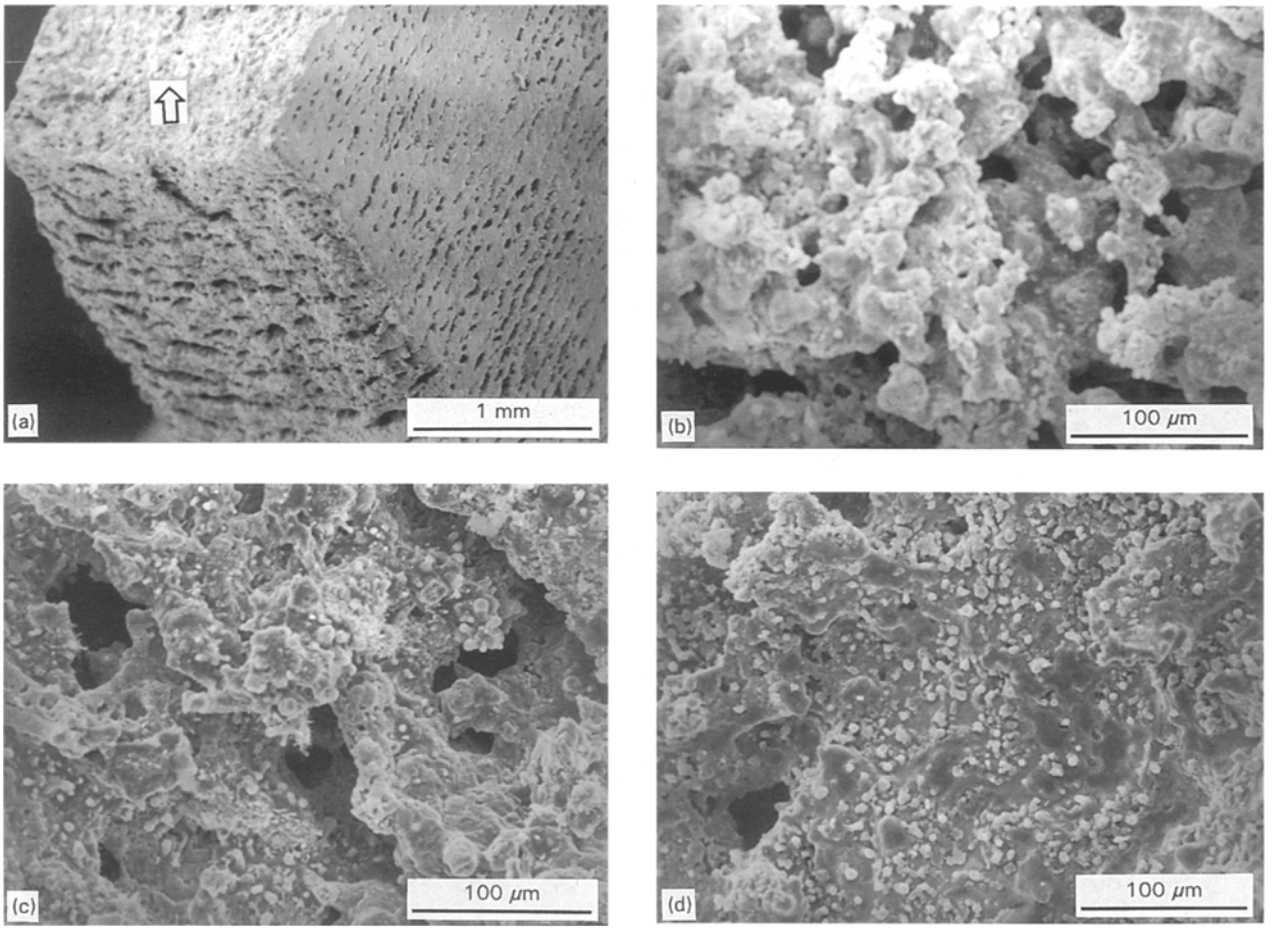

Figure 14 (a) SEM showing orientation of the fracture surfaces in (b)–(d). The fracture surface (indicated by the arrow) is perpendicular to the direction of the combustion wave. (b) No Al diluent. (c) 10 wt % Al diluent. (d) 20 wt % Al diluent. The liquid Al infiltrates the laminates, reducing porosity.

inside the reaction tube which was placed through an induction heating coil. A thermocouple was positioned between the reactant sample and the graphite base and the graphite was heated by the induction heater which heated the reactant compact. When the desired thermocouple temperature was attained the sample was left at that temperature for 30 min to allow the temperature to equilibrate throughout the reactant compact. Water cooled copper coils prevented excessive heating of the borosilicate tube, and the maximum preheating temperature possible was estimated to be 600 °C (to prevent softening of the borosilicate glass).

6.1. Effect of preheating on the stoichiometric reaction

The adiabatic combustion temperature in the presence of preheating is calculated thus,

$$-3\Delta H_{r,298} + \int_{298}^{T_{start}} C_p(3TiO_2 + 4Al + 3C)dT = \int_{298}^{T_{ad}} C_p(3TiC + 2Al_2O_3)dT \quad (5)$$

where T_{start} is the preheating temperature.

Fig. 15 shows adiabatic combustion temperature as a function of preheating temperature for the stoichiometric Reaction 1. It is shown that as T_{start} increases from 298 to 873 K there is a gradual increase in the combustion temperature from 2390 to 2860 K, which is accompanied by a corresponding increase in the wave velocity. As the adiabatic combustion temperature increases the product will take a longer time to cool to the solidification point of alumina (2323 K) and therefore a liquid phase will be present in the product for longer periods. This results in the product densifying as shown by the microstructures in Fig. 16. As the preheating temperature increases the product becomes more dense.

6.2. Effect of preheating on a reaction containing a diluent

When an alumina diluent was added to the reaction the specimen cracked and the laminar structure was no longer observed. This was thought to occur because the combustion temperature was reduced to below the melting point of alumina. This hypothesis can be examined by using preheating to raise the adiabatic combustion temperature of the diluted samples to the adiabatic combustion temperature of the

stoichiometric reaction at room temperature, i.e. above the melting point of alumina at 2390 K. Fig. 17 shows the calculated variation of adiabatic combustion temperature with starting temperature for samples which contain 10 and 20 wt % alumina diluent. For the 10 wt % diluent addition sample, T_{ad} is similar to that of the stoichiometric reaction when the preheating temperature is 400 °C (673 K) and T_{ad} increases to 2550 K when the preheating temperature is 600 °C (873 K). For the 20 wt % diluent sample the adiabatic combustion does not increase to above the melting point of alumina although when T_{start} is 600 °C, 86% of the alumina phase is calculated to have melted. It should be remembered that the 10 wt % sample was severely cracked when ignited at room temperature and that the 20 wt % sample could not be ignited.

The sample compositions and preheats are shown in Table II.

Fig. 18a shows the TiC–Al_2O_3 product of the preheated 20 wt % alumina diluent sample which displays no cracking. In addition, no cracks were observed in the 10 wt % samples which were heated to 400 and 600 °C. These results show the importance in raising the adiabatic combustion temperature to above the melting temperature of one phase in order to relieve the high thermal stresses which develop during the high temperature reaction.

Fig. 18a also shows that a laminar structure in the ceramic is observed and Fig. 18b–d are optical micrographs of the three samples which all show a laminar structure. Although the microstructures are not as regular as found with the stoichiometric reaction they are very different to the microstructures of the diluted samples which were not preheated as seen in Fig. 11. It is therefore possible that a liquid phase is important in the mechanism which produces the laminar structure.

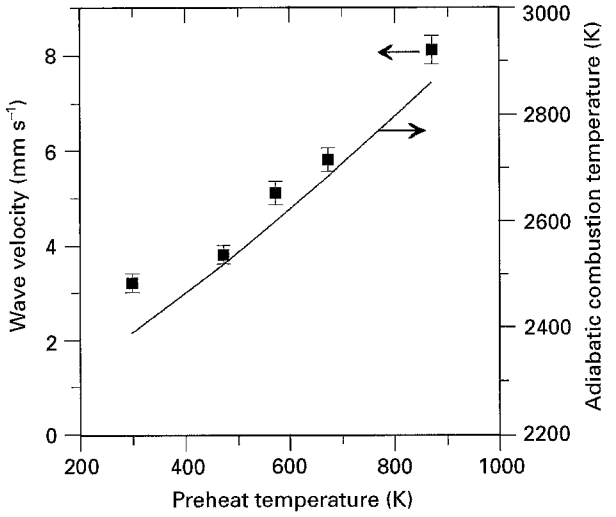

Figure 15 Graph of combustion wave velocity and calculated adiabatic combustion temperature versus preheating temperature.

7. Conclusions

The effects of a variety of processing parameters have been investigated for an SHS reaction. The effect of

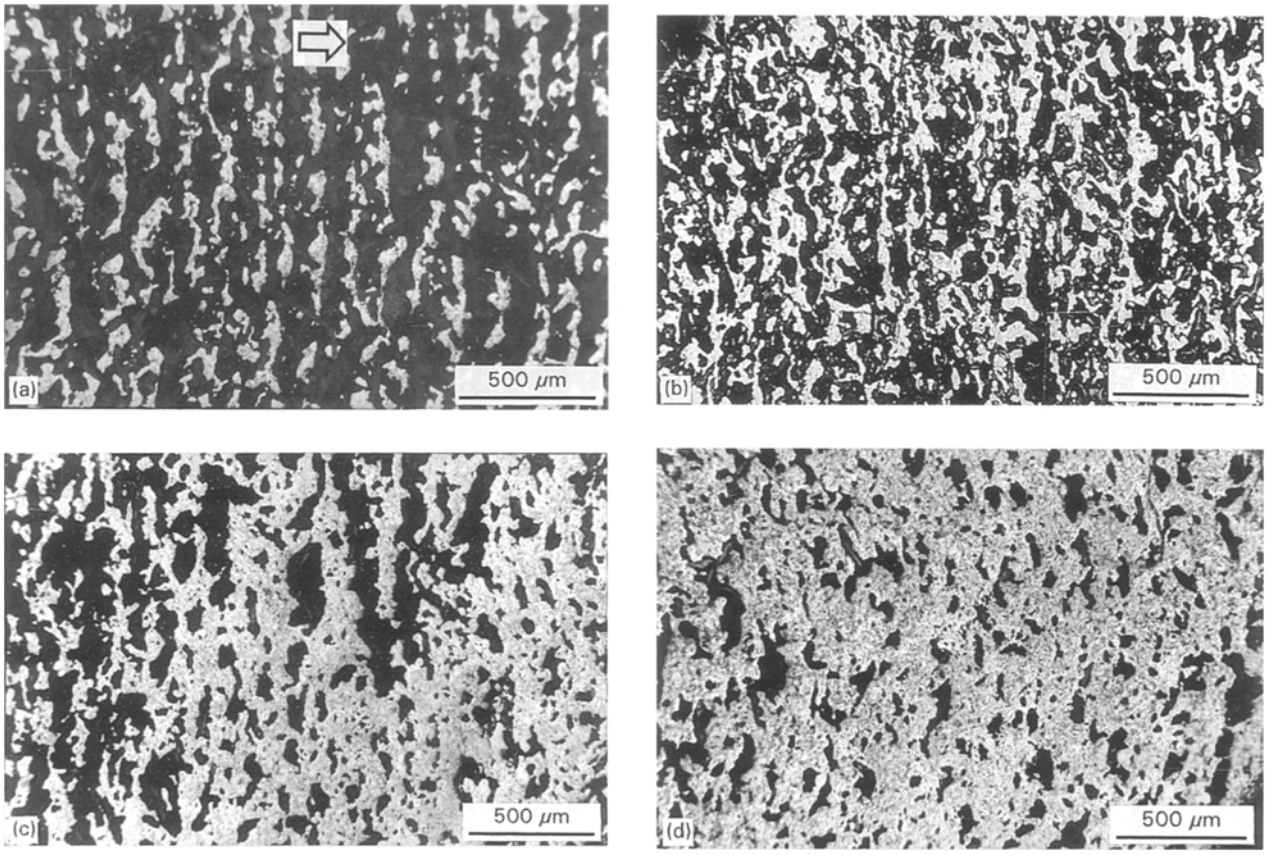

Figure 16 TiC–Al_2O_3 microstructures formed with increasing starting temperature. Direction of combustion wave propagation is indicated by the arrow. (a) T_{start} = 298 K, (b) T_{start} = 473 K, (c) T_{start} = 673 K and (d) T_{start} = 873 K.

particle size on the combustion wave velocity and microstructure of the ceramic has been examined. The microstructure of the ceramic has been shown to be highly dependent on the particle size of each of the reactants. The unusual laminar structure observed with this particular reaction is only produced in a narrow range of small particle sizes. Increasing the particle size produces a ceramic with randomly distributed porosity and also tends to promote cracking in the product. Generally, increasing particle size causes a decrease in the wave velocity. However on increasing the carbon particle size the wave velocity increases when the particle size is increased from 0.02 μm carbon black to 7 μm graphite which may be due to the increased thermal conductivity of the reactant compact. This effect highlights the importance of not only the sizes of the particles but also the relative sizes of the particles as this may produce different reactant particle arrangements and result in different microstructures.

The addition of diluents to control the highly exothermic SHS reactions have been investigated. The

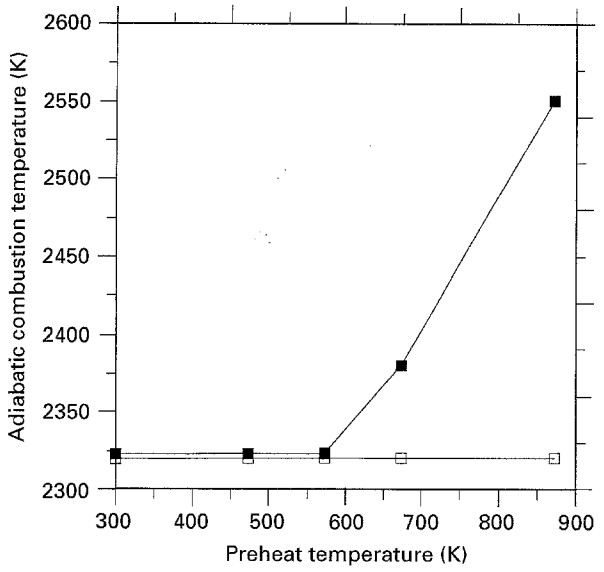

Figure 17 Adiabatic combustion temperatures versus preheating temperature for Reaction 2 containing 10 and 20 wt % Al_2O_3 diluent. Key: ■ 10 wt % alumina diluent; □ 20 wt % alumina diluent.

TABLE II Preheated samples containing an alumina diluent

Al_2O_3 diluent (wt %)	T_{start} (K)	T_{ad} (K)
10	673	2400
10	873	2550
20	873	2323

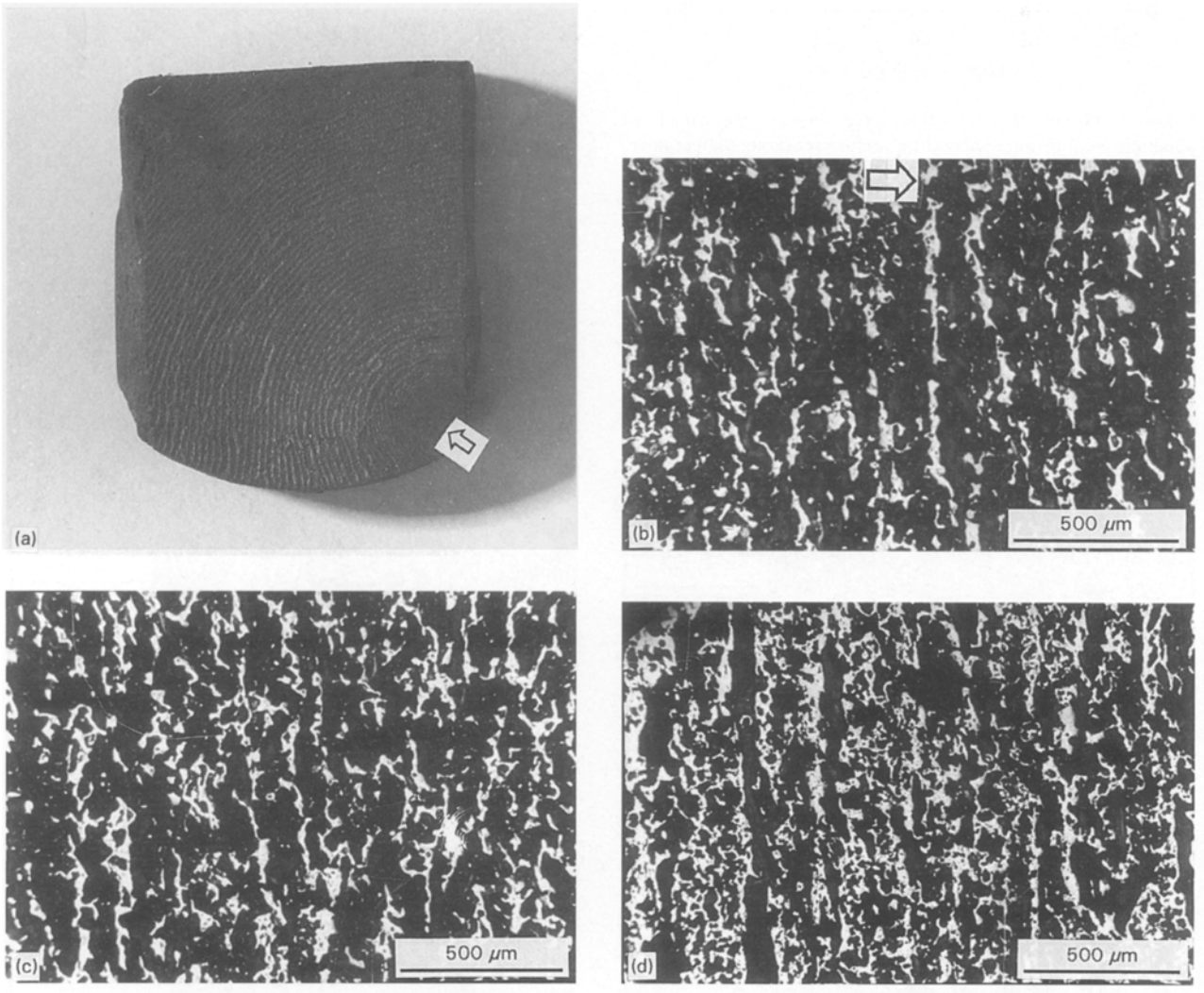

Figure 18 (a) Preheated sample (T_{start} = 873 K) containing 20 wt % Al_2O_3 diluent. No cracking is observed and a laminar structure is produced. Point of ignition is indicated by arrow. (b) 673 K and 10 wt % Al_2O_3 diluent. Direction of combustion wave propagation is indicated by the arrow. (c) T_{start} = 873 K and 10 wt % Al_2O_3 diluent. (d) T_{start} = 873 K and 20 wt % Al_2O_3 diluent.

use of an Al_2O_3 diluent on the reaction $3TiO_2 + 4Al + 3C \rightarrow 3TiC + 2Al_2O_3$ tends to induce cracking in the final product when the combustion temperature falls below the melting point of the alumina phase. As no liquid phase is present during the reaction thermal stresses are not relieved which causes cracking.

The use of aluminium as a diluent produces an unexpected increase in wave velocity with increasing diluent content which could be due to an enhanced diffusion process or heat transfer. The laminar microstructure of the composite is unaffected with large amounts of Al diluent (up to 20 wt %). As the combustion wave is steady and the lamination repeat is independent of wave velocity the formation of the laminates is unlikely to be due to a flame instability mechanism which has been observed elsewhere [9].

Preheating has been employed to increase the reaction rate and combustion wave velocity by increasing the adiabatic combustion temperature of an SHS reaction. By preheating reactants containing Al_2O_3 diluents the adiabatic combustion temperature can be increased to melt the alumina phase, thus preventing cracking of samples and confirming that a liquid phase can allow thermal stresses to be relieved during the high temperature reaction. The laminar microstructure is observed with preheated samples containing alumina diluents (the structure is not seen when $T_{start} = 298$ K). This shows that a liquid phase may be important in the mechanism which produces the laminar structure.

Acknowledgement

The authors would like to thank the SERC and the Cookson Technology Centre for funding the work through a research studentship.

References

1. Z. A. MUNIR and U. ANSELMI-TAMBURINI, *Mater. Sci. Rep.* **3** (1989) 277.
2. H. C. YI and J. J. MOORE, *J. Mater. Sci.* **25** (1990) 1168.
3. L. J. KECSKES and A. NIILER, *J. Amer. Ceram. Soc.* **72** (1989) 655.
4. R. W. RICE and W. J. McDONOUGH, *ibid.* **68** (1985) C122.
5. Y. MIYAMOTO, M. KOIZUMI, S. ADACHI, T. WADA and T. MIHARA, *ibid.* **73** (1990) 1451.
6. R. ABRAMOVICI, *Mater. Sci. Eng.* **71** (1985) 313.
7. C. R. BOWEN and B. DERBY, *Br. Ceram. Proc.* **50** (1991) 29, Fabrication Science and Technology, ed. D. Thompson.
8. W. R. WRZENSKI and J. C. RAWERS, *J. Mater. Sci. Lett.* **9** (1990) 432.
9. S. ZHANG and Z. A. MUNIR, *J. Mater. Sci.* **27** (1992) 5789.
10. R. W. RICE, G. Y. RICHARDSON, J. M. KUNETZ, T. SCHROETER and W. J. McDONOUGH, *Adv. Ceram. Mater.* **2** (1987) 222.
11. C. R. BOWEN and B. DERBY, *J. Therm. Anal.* **42** (1994) 713.
12. C. R. BOWEN, S. HÜLLSMAN and B. DERBY, in Proceedings of the 2nd European Ceramic Society Conference, Augsburg, September 1991, edited by G. Ziegler and H. Hausner (Deutsche Keramische Gesellschaft, Köln, Germany) p. 631.
13. H. J. FENG and J. J. MOORE, High Temperature Materials, edited by W. Johnston and R. A. Rapp (Electrochemical Society, 1990) p. 123.
14. T. KOTTKE, L. J. KECSKES and A. NIILER, *AIChE J.* **36** (1990) 1581.
15. S. D. DUNMEAD, D. W. READEY and C. E. SEMIER, *J. Amer. Ceram. Soc.* **72** (1989) 2318.
16. H. J. FENG, J. J. MOORE and D. G. WIRTH, *Metal Trans. A* **23A** (1992) 2373.
17. Z. Y. FU, R. Z. YUAN, Z. A. MUNIR and Z. L. WANG, *Int. J. SHS* **1** (1992) 119.
18. J. B. HOLT and Z. A. MUNIR, *J. Mater. Sci.* **21** (1986) 251.
19. D. HALVERSON, B. Y. LUM and Z. A. MUNIR, in Symposium on High-Temperature Materials IV at the 172nd Meeting of the Electrochemical Society, Honolulu, edited by Z. A. Munir *et al.* (Electrochemical Society, 1987) p. 613.
20. H. C. YI, A. PERTRIC and J. J. MOORE, *J. Mater. Sci.* **27** (1992) 6797.

Received 6 February
and accepted 4 October 1995